

# A lattice model for the electrical double layer using finite-length dipoles

Stephen W. Kenkel and J. Ross Macdonald

*Department of Physics and Astronomy, University of North Carolina, Chapel Hill, North Carolina 27514*

(Received 1 May 1984; accepted 15 June 1984)

A lattice model of the metal electrode–electrolyte interface is presented which partitions the region into a number of planar layers. In each layer statistical competition occurs between ions and solvent molecules, represented as point charges and finite length dipoles, respectively. Differential capacitance and other results are compared with those of earlier models and with experiments. Agreement with experiments requires explicit inclusion of an inner layer with solvent properties which differ from the remainder of the system. The inner layer may consist of finite-length dipoles alone, or of both dipoles and charges. The use of finite length dipoles drastically changes the high field saturation properties of the layers, as compared with models involving infinitesimal (point) dipoles. Very little dielectric saturation occurs at physically realizable fields.

## I. INTRODUCTION

An adequate analysis of the electrical double layer which forms at the interface between a metal electrode and a liquid electrolyte remains a difficult and intriguing problem. A full theory of this situation should treat both the ions and the solvent molecules discretely, taking into account such effects as finite size, dielectric saturation, and cooperative interaction. We present a layered lattice gas treatment which meets many of these goals, at the price of certain simplifications.

The classical Gouy–Chapman<sup>1,2</sup> treatment of the interface between an electrode and a system of mobile charges involves a model which represents the ions as point charges embedded in a homogeneous dielectric medium. It thus takes no account of the steric interactions between ions which limit the charge density close to the electrode, nor of dielectric saturation which occurs as polar molecules line up with the local field. An improvement is the inclusion of a special charge free inner layer.<sup>3</sup> This prevents the unphysical build up of charge near the electrode. In addition, by taking the dielectric constant of this layer to be small compared to the bulk value, one can take some account of solvation and dielectric saturation.

A less phenomenological approach is to treat the more realistic model system of charged hard spheres in a dielectric continuum by the methods of modern statistical mechanics—usually involving integral equations in terms of the correlation functions.<sup>4–10</sup> Much effort has been expended to enable regions of high charge concentrations and electric fields to be treated. These theories are now in good agreement with simulation results for the simplified model systems. The extension to models in which the solvent molecules are also treated microscopically (e.g., as hard spheres with embedded dipoles) is possible, but yet more difficult.<sup>11–13</sup>

The intractability of these theories is of course the result of a situation which cannot be considered a small perturbation of a simple solved model. For example, in the bulk or diffuse layer, the ordinary Gouy–Chapman theory usually gives good results, indicating that the hard sphere interaction is a minor correction to the basic Poisson–Boltzmann

model. In the region near the electrode, however, both hard-sphere and Coulomb effects are quite important and in direct competition. Statistical treatments are thus usually limited to low fields and/or systems where the solvent difficulties molecules have small dipole moments. One way out of these difficulties is to substitute an artificial lattice for the hard sphere interactions. Earlier work has shown that this approach may be quite useful for liquid electrolytes,<sup>14–21</sup> even though it should be most appropriate for solids. A feature of these models is that the system can be divided into layers parallel to the electrode. The inner layer can thus be treated in the same way as the remainder of the system or special properties can be assigned to it.

## II. THE MODEL SYSTEM

In earlier work<sup>22</sup> we introduced a layered lattice gas model involving point charges and finite length (“dumb-bell”) dipoles. In that work we derived the basic equations, presented exact solutions for a single layer, and determined the dielectric constant of a pure dipole system. We review here the most important features of the theory.

The model consists of point charges, representing the mobile ions, and finite-length dipoles, representing the polar solvent molecules. The model system is divided into planar layers parallel to the electrode. Within each layer the charges and dipoles are restricted to sites on a two-dimensional square lattice, lattice constant  $a$ . The quantity  $a$  corresponds to the hard sphere diameter of the solvent molecules; thus for water we use  $a = 3.1 \text{ \AA}$ . All quantities are averaged over the plane parallel to the electrode layer, so that the electric field, potential, and effective charge density are functions only of the perpendicular distance from the electrode  $x$ . The full system consists of an infinite number of such planar layers. There are  $N_V$  particles (or lattice points) per unit volume. The uni-univalent solute ions each have average concentration  $c_0 = N_V \delta$ . Thus the molarity is  $M_0 \cong c_0 / 6.022 \times 10^{20} \cong 55.5 \delta$ , where  $c_0$  is in number per  $\text{cm}^3$ , and  $M_0$  is mol/l. The  $(1 - 2\delta)N_V$  remaining particles are finite-length dipoles used to represent the solvent molecules. Each dipole consists of two point charges, of magnitude  $\eta e$ , sepa-

rated by a distance  $d = 2t$ . Their permanent dipole moment is  $\mu = \eta ed$ . While it is possible to take the polarizability of the particles into account,<sup>22</sup> we use here instead a homogeneous background dielectric constant  $\epsilon_a = 6.0$ .

The fundamental approach is to solve simultaneously the equations of statistical mechanics, which determine the particle occupancy and dipole orientations as a function of the fields, and the electrostatic equations which link the fields to the ion and dipole numbers and orientations. It is convenient to replace the electric field  $\mathcal{E}$  and the potential  $\psi$  with the normalized potential

$$\phi \equiv \psi/V_N, \tag{1}$$

and the normalized field

$$E(y) \equiv \mathcal{E}(x)/E_N, \tag{2}$$

where

$$V_N \equiv kT/e \equiv E_N t. \tag{3}$$

Here  $y \equiv x/t$  is our normalized distance variable. We use the convention  $E(-1) = E_{-1}$ , etc. The dipole length scales as

$$T_N \equiv t/L_{DN}, \tag{4}$$

where  $L_{DN}$  is the lattice Debye length

$$L_{DN} \equiv [\epsilon_\infty kT/8\pi e^2 N_V]^{1/2}. \tag{5}$$

The normalizing surface charge  $\sigma_N$  and capacitance per unit area  $C_N$  are given by

$$\sigma_N \equiv \epsilon_\infty kT/4\pi et \equiv C_N V_N. \tag{6}$$

When one makes the simplifying assumption that the length of the dipoles is  $d = a$ , the parameter  $\eta$  determines the effective dipole moment. Using water as a typical solvent, one finds there are two ways to fix this value. If we require that the dipoles have the bare dipole moment of a water molecule,  $\mu = 1.84$  D, we choose  $\eta = 0.124$ . This choice leads to a low value for the dielectric constant of a system of dipoles alone. If we require that such a system have the dielectric permittivity of bulk water at 20 °C,  $\epsilon_B = 80.1$ , we find  $\eta = 0.682$ . This is the value used in most of the work reported here. This enhanced dipole moment represents in a crude way the cooperative effects and hydrogen bonding present in the actual solvent. The dielectric properties of a system of finite-length dipoles alone were explored in detail in Ref. 22 and, independently of our work, in Ref. 23.

Equilibrium statistical mechanics is used to determine the ensemble of orientations of the dipoles in each layer. Each dipole can take on any orientation with respect to the external field. The final configuration consists of a distribution of orientations. These orientations give an equivalent charge density—e.g., if the dipoles were completely aligned with the field, they would produce delta functions in charge density at  $y = -1$  and  $y = 1$ .

The basic electrostatic equations for a single layer are

$$E_0 = E_{-1} - Q_{D1} + Q_I/2, \tag{7}$$

$$E_1 = E_{-1} + Q_I, \tag{8}$$

$$\phi_0 = \phi_{-1} - E_{-1} + Q_{D1} + \phi_{D1}, \tag{9}$$

$$\phi_1 = \phi_{-1} - 2E_{-1} + 2Q_{D1} + 2\phi_{D1} - Q_I. \tag{10}$$

Here  $Q_{D1}$  represents the equivalent charge of the dipoles

between  $y = -1$  and  $y = 0$ ,  $Q_I$  represents the ionic charge, etc. These terms are given in Ref. 22 in terms of complicated combinations of elliptic integrals and Jacobean elliptic functions. The fields and potentials of each layer are linked to the next by electrostatic continuity. At the first layer, next to the electrode

$$E_{-1} = Q_m \tag{11}$$

and

$$\phi_{-1} = \phi_a. \tag{12}$$

Here  $Q_m$  is the normalized surface charge on the electrode and  $\phi_a$  is the applied potential difference, relative to  $x = \infty$ .

### III. RESULTS

The full, self-consistent multiple-layer system cannot be solved analytically except in the limit of low applied fields. In this situation the response is linear and the total capacitance,  $C_T \equiv Q_m/\phi_a$  is also the differential capacitance  $C_D \equiv dQ_m/d\phi_a$ . The fields and potentials vary throughout each layer, but from one layer to the next (and thus from the left to the right edges of a single layer) each declines by a constant ratio  $\gamma$ . That is,

$$E_1 = \gamma E_{-1}, \tag{13}$$

$$\phi_1 = \gamma \phi_{-1}. \tag{14}$$

Substituting these expressions into the low field limiting form of the equations relating  $E$  and  $\phi$ ,

$$Q_{1 \rightarrow} \rightarrow -2\delta T_N^2 \sinh(\phi_0)/Z_T \rightarrow -2\delta T_N^2 \phi_0, \tag{15}$$

$$Q_{D1} \rightarrow E_0 [\cosh(\omega_0) - 1], \tag{16}$$

$$\phi_{D1} \rightarrow E_0 [1 - \omega_0^{-1} \sinh(\omega_0)], \tag{17}$$

where

$$\omega_0 = \sqrt{2\eta} T_N \sqrt{1 - 2\delta} \tag{18}$$

gives finally the normalized capacitance  $A$  as

$$A^2 = \frac{\delta T_N^2}{1 + \delta T_N^2} [\omega_0 \coth(\omega_0)]. \tag{19}$$

Figure 1 presents a plot of the molarity or concentration dependence of the total capacitance at low field for the finite-

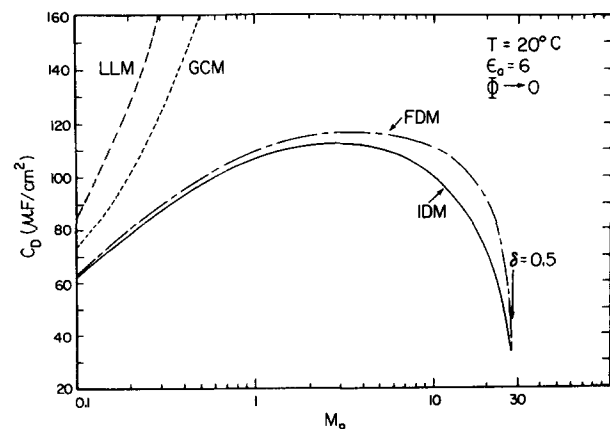


FIG. 1. Low field limiting value of differential capacitance  $C_D$  as a function of molarity for four differential theories: Gouy-Chapman (GC), a liquid lattice model (LLM), an infinitesimal dipole model (IDM), and the present finite dipole model (FDM).

dipole model (FDM). For purposes of comparison we have included results of the Gouy–Chapman,<sup>1,2</sup> theory (GC), that of a liquid lattice model<sup>18</sup> (LLM), and that of a layered model in which the solvent is represented by a region of uniform polarization—equivalent to infinitesimal dipoles<sup>21</sup> (IDM). The layered models do not show the unphysical increase in capacitance at high concentrations that the ideal gas models do. In addition they show the exclusion effect that at high concentration ( $\delta \rightarrow 0.5$ ) there are few dipoles present and thus a low dielectric constant.

For nonzero applied fields there is no analytic solution to the equations above, and they must be solved numerically. The first step is the numerical solution of the single layer equations. Although these equations can be written in closed form, they are implicit—e.g., the equation for the potential involves that potential. A standard nonlinear equation solver package is used to find the combination of field and potential which is self-consistent. Figure 2 shows the fields and potentials in a typical layer. Note particularly that the field at the center of the layer  $E_0$ , has declined by a large factor from that at the left of the layer due to the shielding of the dipoles. This reduction is also present in the mean field approximation treatments of spin dipole models of the inner layer.<sup>25,26</sup> In this case the field acting on a dipole is considered to be the sum of the external field and a reaction field due to the other dipoles. In the small field region the net field may be only about 5% of the external field. In the present model, however, we consider the fields throughout the layer. It is the effect of fields varying over regions of the same size as that of the dipoles that our model particularly attempts to treat.

The more difficult numerical problem is the solution of the full multiple layer system. We find that forward iteration is useful and appropriate. For a given charge on the electrode  $Q_m$  (which determines the field at the left of the first layer) a trial potential  $\phi_a$  is picked. The single layer equations are solved numerically to find the field and potential at the right of this layer, and these values are used as inputs to the next layer. Generally, either the field or potential will become negative or increase within a few layers—showing that the assumed potential is inconsistent with the assumed electrode charge. Then a new guess must be made for the potential.

Iteration continues until a potential is found such that the field decays to  $10^{-6}$  of its initial value before changing sign or increasing. This may require up to 100 layers. This algorithm determines the actual consistent potential to high relative accuracy, on the order of  $10^{-11}$ . As a result of this procedure, the net charge in the system balances that on the electrode and the overall system is very closely electroneutral. Figure 3 shows the way the fields and potentials decline in a multiple layer model. The points represent the parameters at the left edge of each layer, the lines are merely a guide to the eye. Even at relatively high fields, here  $Q_m = 40 \mu\text{C}/\text{cm}^2$  and  $\mathcal{E}_{-1} \sim 7.5 \times 10^7 \text{ V}/\text{cm}$ , the overall curve is nearly a simple exponential decline.

Figure 4 shows the charge on the electrode as a function of the applied potential at different molarities. At the high potential and concentration regions saturation effects appear. These will be treated in more detail in Sec. IV. The differential capacitance curves in Fig. 5 shed more light on the model. Not only is the capacitance different at different molarities, the dependence on electrical field is significantly affected by the bulk concentration.

The above results, while informative and directly comparable to earlier models, are not totally consistent with experiments. Experimental work, such as Grahame's studies of NaF, yields differential capacitances less than  $30 \mu\text{C}/\text{cm}^2$ .<sup>24</sup> The usual explanation is that the layer of solvent molecules nearest to the electrode is qualitatively different from the remaining, diffuse layers. Specifically, the lower capacitance implies a region of low dielectric constant. It is generally assumed that the layer is charge free, following Stern.<sup>3</sup> The inner layer accounts not only for the dipole–dipole interactions, but also reflects the effect of the metal electrode. Theory<sup>27,28</sup> indicates nonlocal effects—the electrical field penetrates the metal surface and the electron wave functions of the metal spill over into the solution. The inner layer capacitance is in series with the bulk capacitance and dominates the total capacitance. It can be treated in several ways. The simplest approach used, e.g., by Macdonald and Liu,<sup>21</sup> is to add a series capacitance to the overall system response. In the more microscopic spirit of this work, we investigate two additional models which incorporate an inner layer with lower dielectric constant. In one case we assume the inner layer to

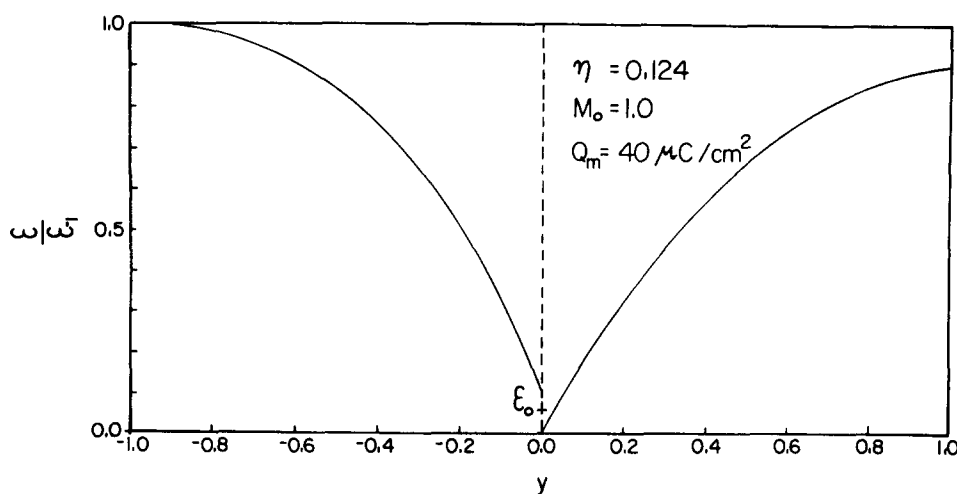


FIG. 2. Relative electric field,  $\mathcal{E}/\mathcal{E}_{-1} = E(y)/E(-1)$ , in a typical layer as a function of distance perpendicular to the electrode  $y$ .

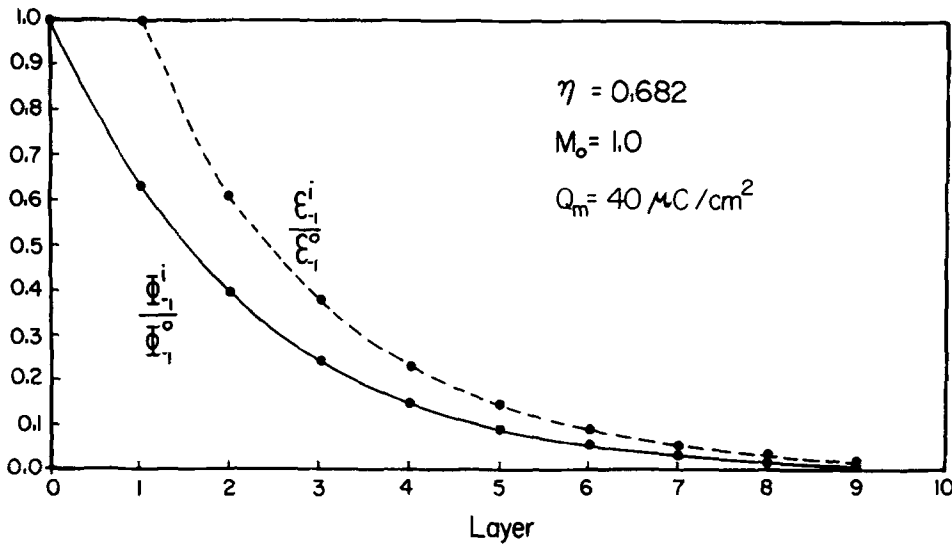


FIG. 3. Electric fields and potentials at the left edge of each layer in a multiple layer model. Data points are marked, lines are a guide to the eye.

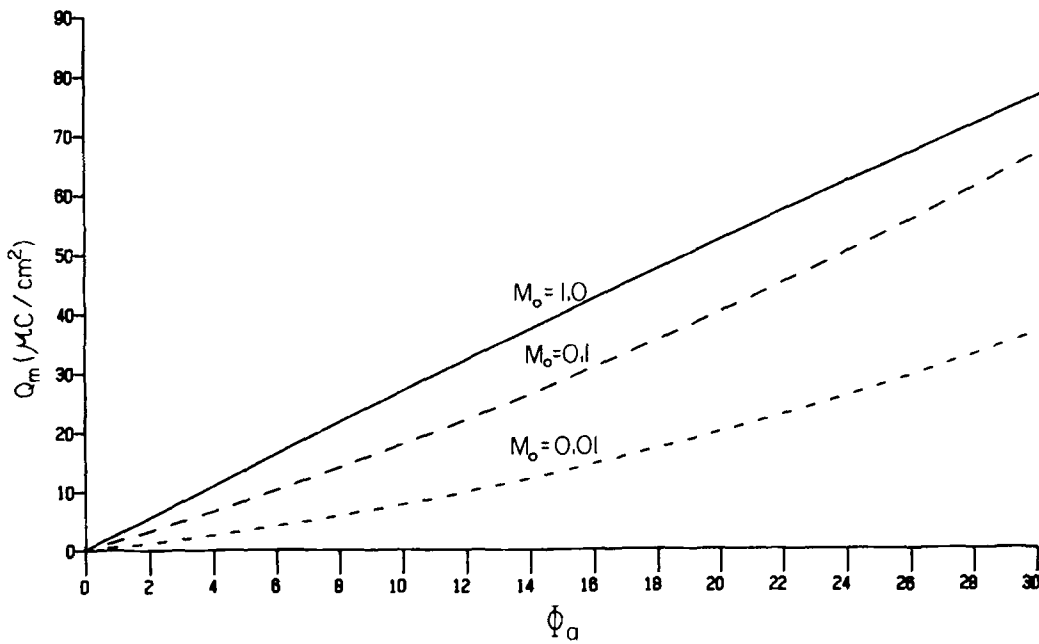


FIG. 4. Normalized surface charge  $Q_M$  as a function of normalized potential  $\phi$  at various molarities.

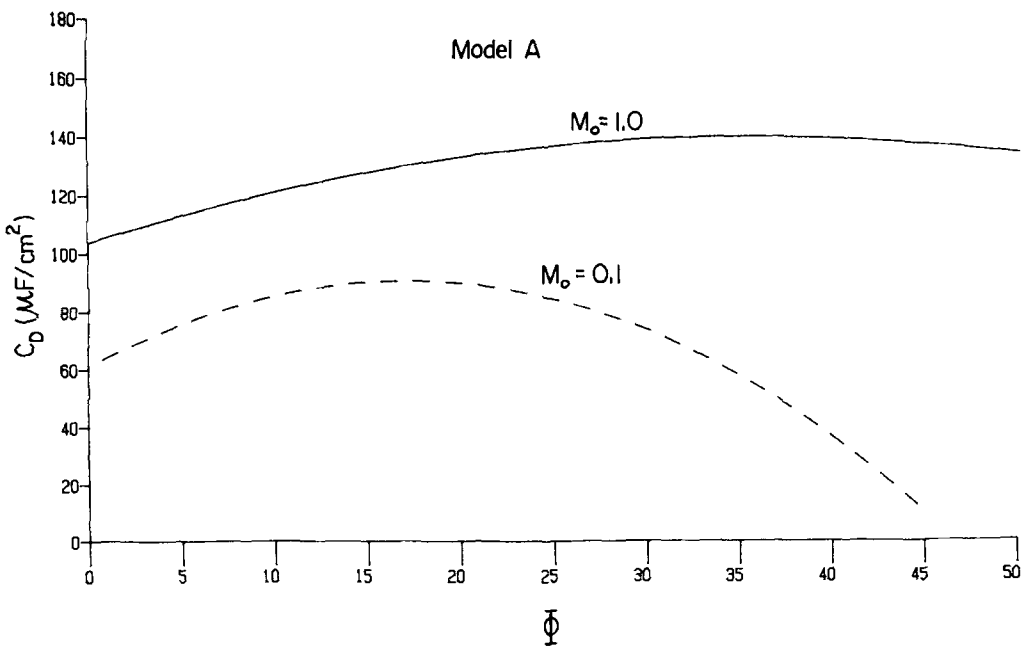


FIG. 5. Differential capacitance as a function of normalized potential for a uniform model, no explicit inner layer.

Table I. Summary of model parameters.

|                            | A     | B     | C     | D          |
|----------------------------|-------|-------|-------|------------|
| $\eta(\text{bulk})$        | 0.682 | 0.682 | 0.124 | 0.682      |
| $\eta(\text{inner layer})$ | ...   | 0.124 | ...   | 0.124      |
| $\delta'$                  | ...   | 0     | ...   | $\delta_b$ |

be charge free but containing dipoles. In the other case we allow charges and dipoles to compete for occupancy in this layer. In both cases the dipole parameter in the inner layer is taken as  $\eta = 0.124$ , corresponding to the bare dipole moment  $\mu = 1.84$  D. This implies that the cooperative effects which enhance  $\eta$  are much reduced in the inner layer. We retain the assumption  $\epsilon_a = 6.0$ .

The low-field value of  $C_T = C_D$  can be calculated in the same way as above. We begin by assuming that the inner layer is charge free. We wish to find a charge and potential at the left side of this layer, such that the charge and capacitance at the right side match the bulk material

$$E_1 = E_{-1}, \quad (20)$$

$$\phi_1 = \gamma\phi_{-1} \quad (21)$$

(the electric field is the same on both sides of the first layer because no net charge is contained in this layer) and

$$E_1/\phi_1 \equiv A_b, \quad (22)$$

where the subscript  $b$  stands for bulk.

A simple calculation gives

$$E_{-1}/\phi_{-1} = A_{\text{eff}} = [A_B^{-1} + K_3]^{-1}, \quad (23)$$

$$K_3 = 2Th \equiv 2 \tanh(\omega_0)/\omega_0. \quad (24)$$

This is equivalent to the addition to the diffuse layer capacitance of a series capacitor of capacitance  $C = 1/K_3$ . In the situation where the inner layer has  $\eta = 0.124$ , but charges

Table II. Low field limiting values of the differential capacitance  $C_D$  for the various models compared to experiment (Ref. 24) ( $E$ ). Capacitance is  $\mu\text{C}/\text{cm}^2$ , concentration is mol/l.

| Concentration | A     | B    | C    | D    | E    |
|---------------|-------|------|------|------|------|
| 1.0           | 109.3 | 30.5 | 47.1 | 30.1 | 26.0 |
| 0.1           | 63.4  | 25.4 | 27.2 | 25.2 | 20.7 |
| 0.01          | 22.9  | 14.8 | 9.8  | 14.8 | 13.1 |

and dipoles are competing for occupancy, we again match the bulk at the right side of the layer. Similar calculations then lead to the result

$$A_{\text{eff}} = \frac{A_b(1 + \delta' + \delta'Th) - 2\delta'}{(1 + \delta' - 3\delta'Th) + 2A_bTh(1 + \delta')}, \quad (25)$$

where  $\delta'$  refers to the zero field ion concentration in the first layer. Note that when  $\delta' \rightarrow 0$ , this result reduces to that of Eq. (23), as it should. Table I summarizes possible choices for the inner layer and the remaining system—enhanced or bare dipole parameter, charge-free inner layer or not. The various choices are indicated by models  $A$ ,  $B$ ,  $C$ , and  $D$ . Table II gives the low field capacitance of each model at three different molarities and the corresponding experimental values.<sup>24</sup> An explicit inner layer of low effective dielectric constant is seen to be necessary.

Figure 6 shows the potential dependence of the differential capacitance with the added inner layer at two different molarities, calculated numerically self-consistently. Again we see that the capacitance is reduced, and the dependence on field is changed by the inner layer. All the capacity curves are symmetric around  $\phi_a = 0$ , which corresponds to the experimental potential of zero charge.

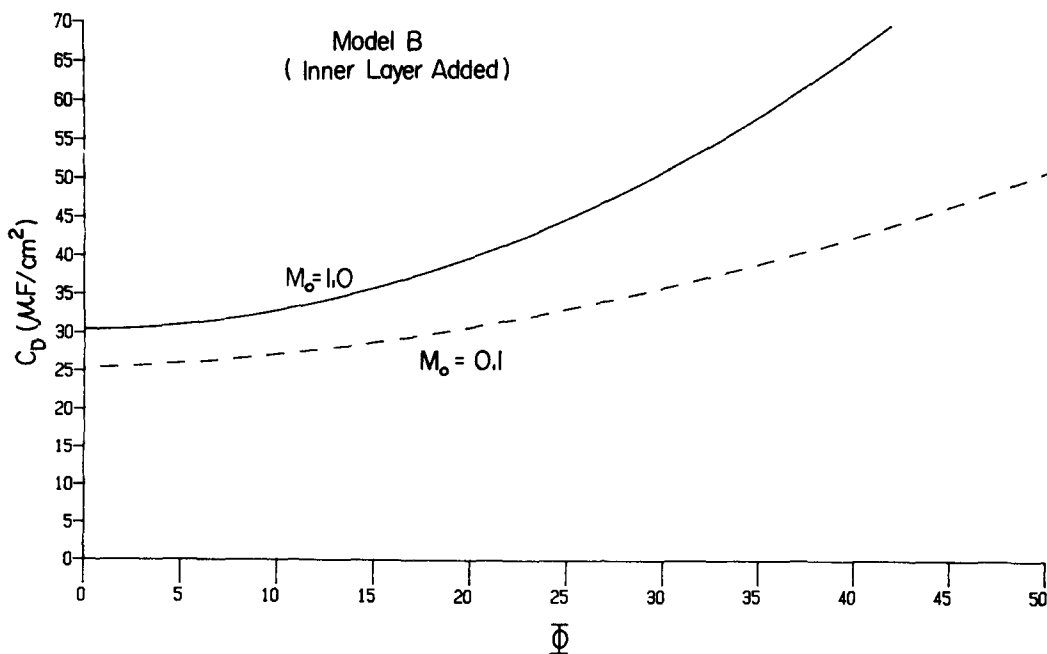


FIG. 6. Differential capacitance as a function of normalized potential in models with an inner layer.

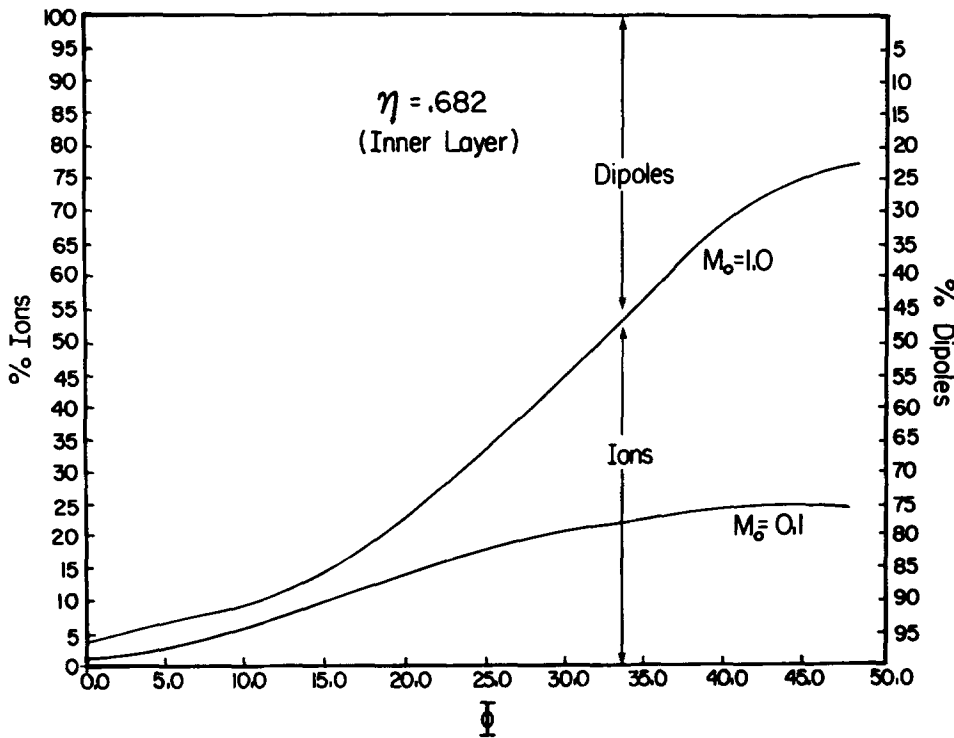


FIG. 7. Competition for site occupancy—percentage of sites in the inner layer occupied by ions and dipoles.  $Q_{\max}$  corresponds to an unnormalized maximum ion charge of  $166 \mu\text{C}/\text{cm}^2$ ,  $Q_{D\max}$  corresponds to an equivalent dipole charge of  $113 \mu\text{C}/\text{cm}^2$ .

#### IV. SATURATION

The present semimicroscopic approach allows us to investigate two different saturation effects. The lattice occupancy restriction limits the maximum charge density in a layer to  $Q_I \leq T_N^2 \equiv Q_{\max}$ . In unnormalized terms,  $\sigma_I \leq 166 \mu\text{C}/\text{cm}^2$ . (The exact numerical value is a function of the square lattice we have assumed. A hcp lattice would imply  $\sigma_I \leq 192 \mu\text{C}/\text{cm}^2$ .) The parameter  $Q_I/Q_{\max}$  is thus a measure of the extent of charge saturation. Figure 7 shows how the percentage of lattice sites in the first layer occupied by ions depends on applied potential. Naturally as ions move into the layer, they crowd out the dipoles.

A second type of saturation is related to the orientation of the permanent dipoles. An appropriate measure of this is

$Q_D$ , the equivalent dipole charge. This parameter is limited by  $Q_D \leq \eta T_N^2 \equiv Q_{D\max}$ .  $Q_D$  measures the effect of the dipoles on the field, and thus includes both the orientation and the number of the dipoles. The maximum value of this parameter occurs when all of the particles in a layer are dipoles, and when all the dipoles are lined up with the field. Figure 8 shows the saturation parameters  $Q_I/Q_{\max}$  and  $Q_D/Q_{D\max}$  for the first layer in a model where both ions and dipoles are competing for occupancy. As established earlier,<sup>21,22</sup> very high fields are required to saturate the finite-length dipoles.

#### VI. CONCLUSIONS

The present work has demonstrated the possibility of using a layered lattice gas model to represent the metal electrode-liquid electrolyte interface. Various finite-size effects can be included in this treatment which are very difficult to add to other models. The most important conclusion, however, is that these effects are not sufficient—a distinct inner layer with properties which differ from the rest of the system is still required. This inner layer represents the effects of specific adsorption, field penetration, and cooperative dipole interactions found at actual interfaces.

Some possible extensions readily suggest themselves. The “average field” approximation is the most severe simplification we have employed. Some further incorporation of lateral local field effects, e.g., an additional mean field, would be most useful. (The present model already incorporates, through its self-consistency, a certain kind of mean field.) The major feature which is left untreated is the cooperative interaction of the solvent dipoles—their tendency to prefer to be either aligned or antialigned.<sup>25,26</sup> Work is in progress to consider these effects, especially in the inner layer.

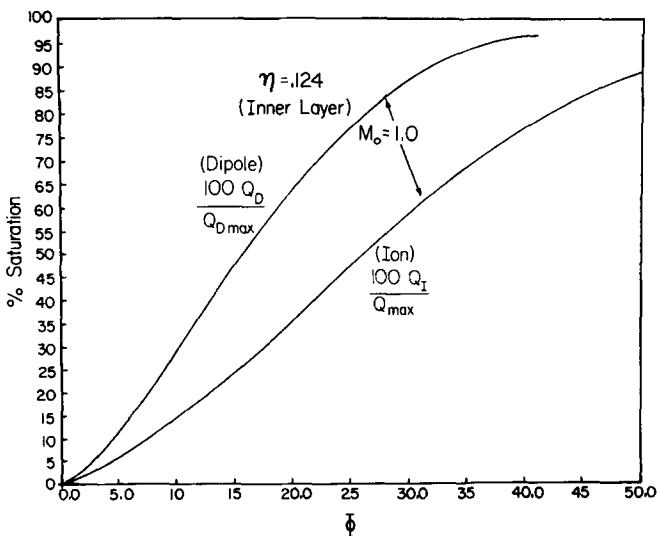


FIG. 8. Ion and dipole saturation  $Q_I/Q_{\max}$  and  $Q_D/Q_{D\max}$  as a function of potential.

**ACKNOWLEDGMENT**

We wish to thank the Army Research Office for support.

- <sup>1</sup>G. Gouy, *J. Phys. Radium* **9**, 457 (1910).  
<sup>2</sup>D. L. Chapman, *Philos. Mag.* **25**, 475 (1913).  
<sup>3</sup>O. Stern, *Z. Electrochem.* **30**, 508 (1924).  
<sup>4</sup>L. Blum, *J. Phys. Chem.* **8**, 136 (1977).  
<sup>5</sup>D. Henderson and L. Blum, *J. Chem. Phys.* **69**, 5441 (1978).  
<sup>6</sup>S. Levine and C. W. Outhwaite, *J. Chem. Soc. Faraday Trans. 2* **74**, 1960 (1978).  
<sup>7</sup>D. Henderson, L. Blum, and W. R. Smith, *Chem. Phys. Lett.* **63**, 381 (1979).  
<sup>8</sup>C. W. Outhwaite, L. B. Vuiyan, and S. Levine, *J. Chem. Soc. Faraday Trans. 2* **76**, 1388 (1980).  
<sup>9</sup>D. Henderson and L. Blum, *Surf. Sci.* **101**, 189 (1980).  
<sup>10</sup>D. Henderson and L. Blum, *Can. J. Chem.* **59**, 1906 (1981).  
<sup>11</sup>D. Henderson and L. Blum, *J. Electroanal. Chem.* **132**, 1 (1982).  
<sup>12</sup>G. P. Morriss and J. W. Peram, *Mol. Phys.* **43**, 670 (1981).  
<sup>13</sup>G. P. Morriss and P. T. Cummings, *Mol. Phys.* **45**, 1099 (1982).  
<sup>14</sup>J. R. Macdonald, D. R. Franceschetti, and A. P. Lehn, *J. Chem. Phys.* **73**, 5272 (1980).  
<sup>15</sup>J. R. Macdonald, *J. Chem. Phys.* **75**, 3155 (1981).  
<sup>16</sup>A. P. Lehn and J. R. Macdonald, *Cryst. Lattice Defects* **9**, 149 (1983).  
<sup>17</sup>J. R. Macdonald, A. P. Lehn, and D. R. Franceschetti, *J. Phys. Chem. Solids* **43**, 39 (1982).  
<sup>18</sup>J. R. Macdonald, D. R. Franceschetti, and A. P. Lehn, *Solid State Ionics* **5**, 105 (1981).  
<sup>19</sup>S. H. Liu, *Surf. Sci.* **101**, 49 (1980).  
<sup>20</sup>J. R. Macdonald, *Surf. Sci.* **116**, 135 (1982).  
<sup>21</sup>J. R. Macdonald and S. H. Liu, *Surf. Sci.* **125**, 653 (1983).  
<sup>22</sup>J. R. Macdonald and S. W. Kenkel, *J. Chem. Phys.* **80**, 2168 (1984). The phrase "permanent dipoles (p.d.)" in the abstract of this paper should be replaced by its unedited original version: "potential difference (p.d.)."  
<sup>23</sup>P. Dalrymple-Alford and K. B. Oldham, *Can. J. Chem.* **56**, 861 (1978).  
<sup>24</sup>D. C. Grahame, *J. Am. Chem. Soc.* **76**, 4819 (1954).  
<sup>25</sup>W. R. Fawcett and R. M. de Nobrega, *J. Phys. Chem.* **86**, 371 (1982).  
<sup>26</sup>W. Schmickler, *J. Electroanal. Chem.* **149**, 15 (1983).  
<sup>27</sup>A. Kornyshev, W. Schmickler, and M. Vorotyntsev, *Phys. Rev. B* **25**, 5244 (1982).  
<sup>28</sup>W. Schmickler and D. Henderson, *J. Chem. Phys.* **80**, 3381 (1984).